

Signals of the QCD Phase Transition in Core-Collapse Supernovae

I. Sagert,¹ T. Fischer,³ M. Hempel,¹ G. Pagliara,² J. Schaffner-Bielich,² A. Mezzacappa,⁴
F.-K. Thielemann,³ and M. Liebendörfer³

¹*Institut für Theoretische Physik, Goethe-Universität, Max-von-Laue-Str. 1, 60438 Frankfurt am Main, Germany*

²*Institut für Theoretische Physik, Ruprecht-Karls-Universität, Philosophenweg 16, 69120 Heidelberg, Germany*

³*Department of Physics, University of Basel, Klingelbergstr. 82, 4056 Basel, Switzerland*

⁴*Physics Division, Oak Ridge National Laboratory, Oak Ridge, Tennessee 37831, USA*

(Received 12 August 2008; published 26 February 2009)

We explore the implications of the QCD phase transition during the postbounce evolution of core-collapse supernovae. Using the MIT bag model for the description of quark matter, we model phase transitions that occur during the early postbounce evolution. This stage of the evolution can be simulated with general relativistic three-flavor Boltzmann neutrino transport. The phase transition produces a second shock wave that triggers a delayed supernova explosion. If such a phase transition happens in a future galactic supernova, its existence and properties should become observable as a second peak in the neutrino signal that is accompanied by significant changes in the energy of the emitted neutrinos. This second neutrino burst is dominated by the emission of antineutrinos because the electron degeneracy is reduced when the second shock passes through the previously neutronized matter.

DOI: [10.1103/PhysRevLett.102.081101](https://doi.org/10.1103/PhysRevLett.102.081101)

PACS numbers: 26.50.+x, 21.65.Qr, 26.60.-c, 95.85.Ry

In search of the phase transition from hadronic to deconfined matter, heavy-ion experiments at RHIC and at LHC explore the QCD phase diagram for large temperatures and small baryochemical potentials—conditions, which were also present in the early universe. For high chemical potentials and low temperatures a first order chiral phase transition is expected and will be tested at the FAIR facility at GSI Darmstadt. Because of their large central densities, compact stars can also serve as laboratories for nuclear matter beyond saturation density and may contain quark matter [1]. The formation of quark matter in compact stars is mainly discussed in two scenarios, in protoneutron stars (PNSs) after the supernova explosion [2] and in old accreting neutron stars [3,4].

In this Letter we follow a third and less discussed case. The phase transition from hadronic to quark matter can already occur in the early postbounce phase of a core-collapse supernova [5–9]. This requires a phase transition onset close to saturation density, which can be realized for high temperatures and low proton fractions. For such a scenario Ref. [7] found the formation of a second shock as a direct consequence of the phase transition. However, the lack of neutrino transport in their model allowed them to investigate the dynamics only for a few ms after the bounce. Recently, a quark matter phase transition has been considered with Boltzmann neutrino transport for a $100M_{\odot}$ progenitor [10]. The appearance of quark matter shortened the time until black hole formation but did not lead to the launch of a second shock.

In our core-collapse simulations of low- and intermediate-mass progenitor stars, we confirm the formation of a second shock caused by the phase transition to quark matter. We even find that the second shock triggers a delayed supernova explosion during the postbounce accre-

tion phase. This represents an interesting addition to currently discussed supernova explosion mechanisms, such as the neutrino-driven [11], the magneto-rotational [12,13] or the acoustic mechanisms [14]. A clear imprint of the phase transition to quark matter at the launch of the explosion could be expected in the neutrino signal, the emission of gravitational waves [3,4], and the nucleosynthesis yields.

Lattice QCD is not yet able to make predictions for large chemical potentials relevant for neutron star calculations. Consequently, the quark matter equation of state (EOS) is currently computed using phenomenological descriptions such as the MIT bag or the NJL models. As we aim to study the basic effects from quark matter phase transitions on core-collapse supernovae, we chose the very simple but widely applied MIT bag model. In modeling the phase transition to quark matter there is a main physical uncertainty: the critical density n_{crit} for the onset of the mixed phase. In our model, n_{crit} is determined by the bag constant B and the strange quark mass. At present, the bag constant is not a fixed parameter, with typical values between $B^{1/4} = 145\text{--}200$ MeV [15]. We choose the bag constant such that we obtain an early onset for the phase transition and a maximum mass of more than $1.44M_{\odot}$, without enabling absolutely stable strange quark matter. In compliance with these constraints we select $B^{1/4} = 162$ MeV (*eos1*) and 165 MeV (*eos2*), and a strange quark mass of 100 MeV as indicated by the Particle Data Group [16]. For the hadronic EOS we use the table of Shen *et al.* [17]. The phase transition to quark matter is modeled by a Gibbs construction as discussed in Refs. [8,10]. For comparison, we have also computed the EOS by using the Maxwell construction and find that the results of our core-collapse simulations are qualitatively similar. For the sake of simplicity, we have neglected finite size effects and Coulomb

interactions within the mixed phase. The phase diagram using *eos1* for different proton fractions Y_p is shown in Fig. 1. The two choices of the bag constants lead to critical densities of $\sim 0.12 \text{ fm}^{-3}$ and $\sim 0.16 \text{ fm}^{-3}$, respectively, (for $T = 0$ and a proton fraction $Y_p = 0.3$). We note that the small obtained values for the critical density close to saturation density are not in contradiction with heavy-ion data [18]. In contrast to heavy-ion collisions, high-density supernova matter is isospin asymmetric with a proton fraction $Y_p \sim 0.3$. Furthermore the time scales considered in the postbounce evolution are long enough to establish equilibrium with respect to weak interactions that change the strangeness on the time scales of microseconds or less. The additional strange quark degree of freedom and the large asymmetry energy allow one to obtain small values for n_{crit} and lead to an early appearance of quark matter (see Fig. 1). Our choice of parameters is also compatible with the still most precise neutron star mass measurement of $1.44M_\odot$ for the Hulse-Taylor pulsar [19]. With *eos1* and *eos2*, we obtain values for the maximum gravitational mass of 1.56 and $1.50M_\odot$, respectively. Note that higher neutron star masses can be achieved with more sophisticated models of quark matter [20]. For $B^{1/4} = 162$ and 165 MeV, almost the entire star is composed of quark matter, surrounded by a mixed quark-hadronic phase, which is enclosed by a thin pure hadronic crust.

For the accurate prediction of the three-flavor neutrino signal, general relativistic effects may be important. Hence, we choose for our investigation a well-tested general relativistic description of the neutrino radiation hydrodynamics in spherical symmetry, that is based on Boltzmann neutrino transport [21,22]. Quark matter appears only in optically thick regimes where neutrinos are in thermal and chemical equilibrium with matter, so that the results are independent of the precise value for quark-neutrino interaction rates. Therefore, we use hadronic weak interaction rates [23] in the quark phase and derive the hadron chemical potentials from the quark chemical potentials such that weak equilibrium for neutrinos in quark matter is obtained. Our simulations are launched from a 10 and a $15M_\odot$ progenitor model from Ref. [24].

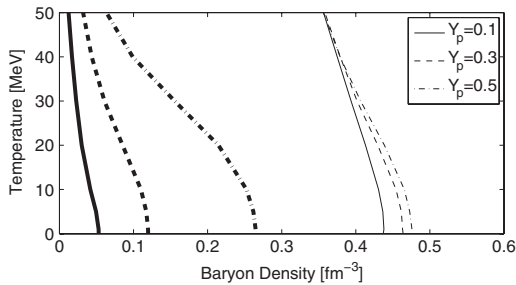


FIG. 1. The onset (thick lines) and the end (thin lines) of the mixed phase from the QCD phase transition from nuclear matter to quark matter using *eos1*.

The standard core-collapse scenario leads to core bounce at nuclear saturation density and the formation of a shock. This expanding shock loses energy due to the dissociation of nuclei and the emission of the ν_e burst at ~ 10 ms after the bounce [see Fig. 2(a)] and therefore turns into a standing accretion shock (SAS). The SAS could be revived by neutrino heating [11]. However, explosions in spherically symmetric models with accurate neutrino transport have only been obtained for a $8M_\odot$ ONeMg progenitor star [25]. The collapse of more massive progenitors leads to an extended postbounce phase, during which the central PNS contracts due to mass accretion. In our models the onset of the quark-hadronic mixed phase is already achieved at the core bounce ($n_B \sim 0.1 \text{ fm}^{-3}$, $T \approx 10$ MeV, $Y_p \sim 0.3$). After remaining small during the first 50 ms the quark matter fraction rises and an increasing central region of the PNS enters the mixed phase. The reduced adiabatic index causes the PNS to collapse.

PNS collapse.—At a central density of 4–5 times nuclear saturation density the collapse halts due to the stiffening of the EOS in the pure quark phase. A large fraction of the PNS is composed out of quarks, enclosed by a mixed hadronic-quark phase, which is surrounded by the infalling hadronic envelope (see Table I). The mixed phase region shrinks gradually during the PNS’s collapse as more and more matter converts from the mixed into the pure quark phase. On this short time scale of ~ 1 ms, the SAS remains almost unaffected by this dynamical evolution inside the

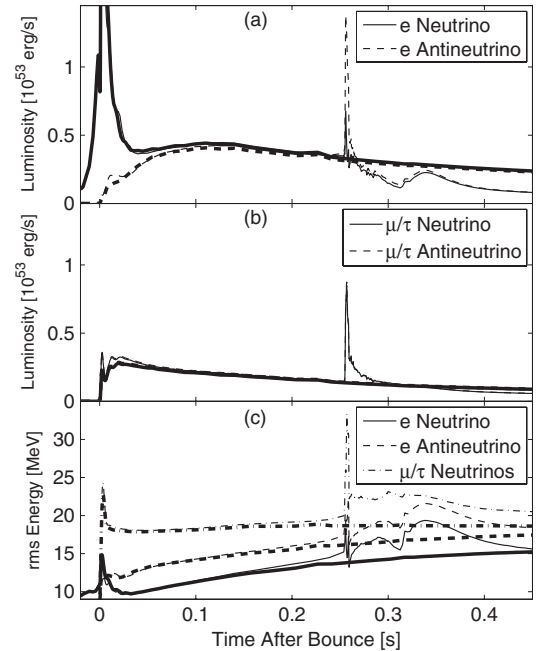


FIG. 2. Neutrino luminosities (a) and (b) and rms-energies (c) calculated at 500 km radius for a $10M_\odot$ progenitor model. The results of the quark EOS *eos1* (thin lines) are compared to the results of the pure hadronic EOS [17] (thick lines). A second neutrino burst is clearly visible at ~ 260 ms after the bounce.

PNS (see Fig. 3). However, the change in the chemical potentials and the increasing density during the phase transition establish weak equilibrium at a lower electron fraction $Y_e \leq 0.1$.

Shock formation and early shock propagation.—A subsonic accretion front forms at the interface between the hydrostatic pure quark phase and the infalling mixed phase (thick dashed line Fig. 3). The accretion front propagates through the mixed phase, meets the supersonically infalling hadrons at the sonic point and turns into an accretion shock (thick dash-dotted line). The high temperature and density at the shock front lead to a rapid conversion of hadronic matter into the mixed phase. As the accreted layers become less dense, the second accretion shock detaches from the mixed phase boundary and propagates into the pure hadronic phase. This phase was deleptonized by the continued emission of electron neutrinos after the first neutronization burst. Weak equilibrium is achieved at $Y_e \sim 0.1$. When the second shock runs across this matter, the electron degeneracy is reduced by shock heating and the weak equilibrium is restored at higher values of the electron fraction ($Y_e \geq 0.2$). The larger adiabatic index of the hadronic phase turns the accretion shock into a dynamic shock with positive matter velocities (see thin solid line Fig. 3).

Explosion.—As the second shock propagates across the steeply declining density gradient in the outer layers of the PNS the shock wave is strongly accelerated. Up to this point, neutrino transport plays a negligible role since neutrinos are trapped. This changes when the second shock reaches the neutrino spheres. A second neutrino burst of all neutrino flavors is released (see Fig. 2), dominated by $\bar{\nu}_e$ stemming from positron captures that establish the above-mentioned increase in Y_e . Because of its compactness the PNS releases (μ/τ) neutrinos with significantly higher mean energies as illustrated in Fig. 2(c). As soon as the expanding second shock merges with the outer SAS, the scenario resembles the situation of a neutrino-driven explosion mechanism (thin dashed line in Fig. 3), except for the large matter outflow with velocities $\sim 10^5$ km/s.

TABLE I. Baryon masses of the quark core, M_Q , the mixed phase, M_{mix} , and the total PNS, M_{pns} , in a late stage when the explosion energies, E_{expl} , are positive. BE is the binding energy of the corresponding cold hybrid star and M_G its gravitational mass. The pure quark phase first appears at postbounce time t_{pb} .

| Prog. | EOS | t_{pb} | M_Q | M_{mix} | M_{pns} | E_{expl} | BE | M_G |
|---------------|-------------|------------------|---------------|------------------|------------------|-------------------|------------------|---------------|
| [M_\odot] | | [ms] | [M_\odot] | [M_\odot] | [M_\odot] | [10^{51} erg] | [10^{53} erg] | [M_\odot] |
| 10 | <i>eos1</i> | 255 | 0.850 | 0.508 | 1.440 | 0.44 | 3.40 | 1.25 |
| 10 | <i>eos2</i> | 448 | 1.198 | 0.161 | 1.478 | 1.64 | 3.19 | 1.30 |
| 15 | <i>eos1</i> | 209 | 1.146 | 0.320 | 1.608 | 0.42 | 4.08 | 1.38 |
| 15 | <i>eos2</i> | 330 ^a | 1.496 | 0.116 | 1.700 | ... ^b | 4.28 | 1.46 |

^amoment of black hole formation

^bblack hole formation before explosion

Behind the expanding matter, a region with matter inflow develops due to neutrino cooling (thin dash-dotted line). The matter inflow becomes supersonic and produces another standing accretion shock at the surface of the PNS at a radius ~ 50 km. The corresponding accretion luminosity explains the transient increase of the electron neutrino flavor luminosities in Fig. 2(a) ~ 340 ms after the bounce. The neutrinos emitted from this cooling region are partly absorbed behind the expanding shock. After the onset of the explosion the neutrino luminosities decrease again.

In general, the models with *eos1* and *eos2* evolve in a qualitatively similar manner. However, the models with the larger bag constant show a longer PNS accretion time before the onset of the phase transition due to the larger critical density. This results in a more massive PNS with a steeper density cliff at its surface. The higher postshock internal energy and the larger density gradient lead to a stronger second shock acceleration at the density cliff and explain the larger explosion energies. In comparison to the simulations using *eos1*, the second neutrino burst appears several 100 ms later and is found to have a larger peak luminosity. The more massive progenitor stars give an earlier onset of the phase transition and result in a more massive PNS with a shallower density cliff. A special case is the dynamical evolution of the PNS of the $15M_\odot$ progenitor model using *eos2*. Almost simultaneously with the formation of the second shock, the more compact quark core collapses to a black hole.

The goal of this investigation is to predict the general effects of a phase transition to quark matter in core-collapse supernovae. The main result is a strong signature of the formation of quark matter, if it occurs during the postbounce phase. A second shock forms inside the PNS, that affects significantly the properties of the emitted neutrinos. For a Galactic core-collapse supernova, a second neutrino burst should be resolvable by the present neutrino detectors. Unfortunately, the time sequence of the neutrino events from SN 1987 A [26] was statistically not significant. While the binding energies of the remaining cold hybrid stars are in agreement with theoretical estimates for the energy release in SN 1987 A [27] further analysis

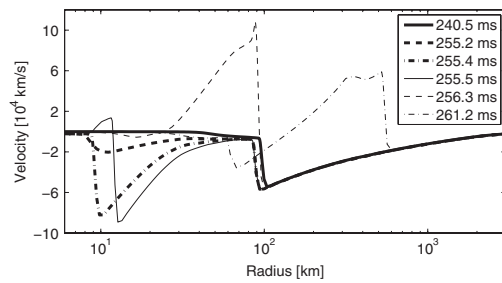


FIG. 3. Velocity profiles at different times during the post-bounce evolution of a $10M_\odot$ progenitor model based on *eos1*, illustrating the development of the explosion through different stages.

and improvements of the EOS would be required to reproduce the temporal structure of the neutrino signal. The magnitude and the time delay of the second neutrino burst provide correlated information about the critical density, the EOS in different phases, and the progenitor model. For low and intermediate mass progenitor models, the energy of the second shock becomes sufficient to drive an explosion even in spherical symmetry. We obtain explosion energies of several 10^{50} erg (see Table I). The explosion is powered by the accretion of matter into the deep gravitational potential followed by the shock acceleration at the surface of the PNS. The ejecta contain neutron-rich material that expands on a fast time scale and should be investigated as a possible site for the r process. With respect to the remnant, the narrow range of PNS masses found in Table I may provide an explanation for the clustering of the observed neutron star masses (gravitational) around $1.4M_{\odot}$ [19]. The discussed direct black hole formation at the phase transition could be investigated further in light of the observed connection between supernovae and γ -ray bursts [28–30].

The presented analysis should be complemented by multidimensional simulations, to explore the impact of known fluid instabilities that cannot be treated in spherical symmetry. Another interesting scenario would be a weak neutrino-driven explosion, followed by a fallback-induced QCD phase transition. Since the QCD phase diagram shows a large variety of color-superconducting phases [31,32], a more sophisticated quark matter EOS should be adopted. This could lead to a second phase transition within the quark core of the PNS and would be an interesting extension of the present study.

This work has been supported by the Swiss National Science Foundation under the Grants No. PP002-106627/1 and No. PP200020-105328/1, the Helmholtz Research School for Quark Matter Studies, the Italian National Institute for Nuclear Physics, the ExtreMe Matter Institute (EMMI), the Frankfurt Institute for Advanced Studies, the German Research Foundation (DFG) within the framework of the excellence initiative through the Heidelberg Graduate School of Fundamental Physics, and by the ESF CompStar program. A. M. is supported at the Oak Ridge National Laboratory, which is managed by UT-Battelle, LLC for the U.S. Department of Energy under Contract No. DE-AC05-00OR22725. We would like to thank D. Blaschke, A. Drago, G. Martínez-Pinedo, and S. C. Whitehouse for stimulating discussions.

[1] F. Weber, Prog. Part. Nucl. Phys. **54**, 193 (2005).

[2] J. A. Pons, A. W. Steiner, M. Prakash, and J. M. Lattimer, Phys. Rev. Lett. **86**, 5223 (2001).

- [3] L.-M. Lin, K. S. Cheng, M. C. Chu, and W. M. Suen, Astrophys. J. **639**, 382 (2006).
- [4] E. B. Abdikamalov, H. Dimmelmeier, L. Rezzolla, and J. C. Miller, arXiv:astro-ph/0806.1700.
- [5] M. Takahara and K. Sato, Astrophys. J. **335**, 301 (1988).
- [6] M. Takahara and K. Sato, Prog. Theor. Phys. **80**, 861 (1988).
- [7] N. A. Gentile, M. B. Aufderheide, G. J. Mathews, F. D. Swesty, and G. M. Fuller, Astrophys. J. **414**, 701 (1993).
- [8] A. Drago and U. Tambini, J. Phys. G **25**, 971 (1999).
- [9] N. Yasutake, K. Kotake, M.-a. Hashimoto, and S. Yamada, Phys. Rev. D **75**, 084012 (2007).
- [10] K. Nakazato, K. Sumiyoshi, and S. Yamada, Phys. Rev. D **77**, 103006 (2008).
- [11] H. A. Bethe and J. R. Wilson, Astrophys. J. **295**, 14 (1985).
- [12] J. M. LeBlanc and J. R. Wilson, Astrophys. J. **161**, 541 (1970).
- [13] G. S. Bisnovatyi-Kogan, Sov. Astron. **14**, 652 (1971).
- [14] A. Burrows, E. Livne, L. Dessart, C. D. Ott, and J. Murphy, New Astron. Rev. **50**, 487 (2006).
- [15] K. Schertler, C. Greiner, J. Schaffner-Bielich, and M. H. Thoma, Nucl. Phys. A **677**, 463 (2000).
- [16] S. Eidelman *et al.* (Particle Data Group), Phys. Lett. B **592**, 1 (2004).
- [17] H. Shen, H. Toki, K. Oyamatsu, and K. Sumiyoshi, Nucl. Phys. A **637**, 435 (1998).
- [18] I. Sagert, G. Pagliara, M. Hempel, and J. Schaffner-Bielich, J. Phys. G **35**, 104079 (2008).
- [19] J. M. Lattimer and M. Prakash, Science **304**, 536 (2004).
- [20] M. Alford *et al.*, Nature (London) **445**, E7 (2007).
- [21] A. Mezzacappa and S. W. Bruenn, Astrophys. J. **410**, 740 (1993).
- [22] M. Liebendörfer, O. E. B. Messer, A. Mezzacappa, S. W. Bruenn, C. Y. Cardall, and F.-K. Thielemann, Astrophys. J. Suppl. Ser. **150**, 263 (2004).
- [23] S. W. Bruenn, Astrophys. J. Suppl. Ser. **58**, 771 (1985).
- [24] S. E. Woosley, A. Heger, and T. A. Weaver, Rev. Mod. Phys. **74**, 1015 (2002).
- [25] F. S. Kitaura, H.-T. Janka, and W. Hillebrandt, Astron. Astrophys. **450**, 345 (2006).
- [26] K. S. Hirata *et al.*, Phys. Rev. D **38**, 448 (1988).
- [27] H. A. Bethe, Rev. Mod. Phys. **62**, 801 (1990).
- [28] Z. Berezhiani, I. Bombaci, A. Drago, F. Frontera, and A. Lavagno, Astrophys. J. **586**, 1250 (2003).
- [29] T. Piran, Rev. Mod. Phys. **76**, 1143 (2005).
- [30] I. N. Mishustin, M. Hanauske, A. Bhattacharyya, L. M. Satarov, H. Stöcker, and W. Greiner, Phys. Lett. B **552**, 1 (2003).
- [31] S. B. Ruster, V. Werth, M. Buballa, I. A. Shovkovy, and D. H. Rischke, Phys. Rev. D **72**, 034004 (2005).
- [32] F. Sandin and D. Blaschke, Phys. Rev. D **75**, 125013 (2007).